

## Supplemental material

### **Bardet-Biedl Syndrome proteins regulate intracellular signaling and neuronal function in patient-specific iPSC-derived neurons**

JCI: Research revised (146287-JCI-RG-RV-3)

Liheng Wang<sup>1,2†</sup>, Yang Liu<sup>3\*</sup>, George Stratigopoulos<sup>1,4\*</sup>, Sunil Panigrahi<sup>1,2</sup>, Lina Sui<sup>1,4</sup>, Charles A. Leduc<sup>1,4</sup>, Hannah J. Glover<sup>1,4</sup>, Maria Caterina De Rosa<sup>1,4</sup>, Lisa C. Burnett<sup>1,5</sup>, Damian J. Williams<sup>6</sup>, Linshan Shang<sup>1,7</sup>, Robin Goland<sup>1</sup>, Stephen H. Tsang<sup>8,9,10</sup>, Sharon Wardlaw<sup>1,2</sup>, Dieter Egli<sup>1,3,11</sup>, Deyou Zheng<sup>3,12</sup>, Claudia A. Doege<sup>1,9,10†</sup>, Rudolph L. Leibel<sup>1,4†</sup>

†Address correspondence to: Liheng Wang, 1150 St. Nicholas Avenue, Room 234, New York, NY 10032, USA. Phone: 212.851.5333; Email: [lw2381@cumc.columbia.edu](mailto:lw2381@cumc.columbia.edu). Or to Claudia A. Doege for cell line request, 1150 St. Nicholas Avenue, Room 620A, New York, NY 10032, USA. Phone: 212.851.5315; Email: [cad2114@cumc.columbia.edu](mailto:cad2114@cumc.columbia.edu). Or to: Rudolph Leibel, 1150 St. Nicholas Avenue, Room 620A, New York, NY 10032, USA. Phone: 212.851.5315; E-mail: [rl232@cumc.columbia.edu](mailto:rl232@cumc.columbia.edu).

## Supplemental figures

**Figure S1. BBS patients - phenotype and genotype.** (A-B) Clinical phenotypes of BBS subject *BBS1B* includes obesity, retinitis pigmentosa (A), polydactyly (B), cognitive impairment and renal cysts. Arrow points to the scar after surgery to remove the extra digit. (C) Dideoxy-sequencing confirming the mutations identified by genetic testing or genome sequencing in four BBS subjects. Red arrows indicate mutation sites.

**Figure S2. *BBS10A* iPSC line is pluripotent and has a normal karyotype.**

(A) Immunocytochemistry analysis of *BBS10A* iPSC line with pluripotency markers as indicated. Scale bar, 200 $\mu$ m; (B) H&E staining of *BBS10A* iPSC-derived teratoma sections. Cell types representing all three germ layers in iPSC-derived teratoma were identified. Scale bar, 200 $\mu$ m. (C) *BBS10A* iPSC had a normal karyotype.

**Figure S3. Reprogramming re-activates endogenous pluripotency genes and silences exogenous genes in iPSCs.**

(A) Expression of endogenous stem cell markers: *SOX2*, *OCT4*, *KLF4*, *c-MYC* and *NANOG* in indicated iPSC lines (passage 8-10) (n=1). Human embryonic stem cell line HUES42 was used as a positive control for endogenous stem cell gene expression; (B) Expression of retroviral genes in reprogrammed iPSC as indicated. 293 cells transduced with retroviral cocktail for 48 hours were used as a positive control for viral gene expression. HUES42 was used as a negative control (n=1).

**Figure S4. Generation of isogenic control iPSC line (c-*BBS1B*) using CRISPR/Cas9.**

(A) Schematic of targeting the *BBS1* locus. Sequence of genomic DNA around the mutation site in *BBS1M390R* before (top) and after (bottom) CRISPR-Cas9 correction. Sequence of guide RNA (gRNA) for *BBS1 M390R* indicated in yellow. Red rectangle marks the mutation. Star marks the silent mutation introduced to avoid cutting of the repair oligo. (B) Dideoxy-sequencing after TOPO cloning confirmed the homozygous correction of *BBS1M390R* mutation in the isogenic control line referred to as c-*BBS1B*. (C) *BBS1B* and c-*BBS1B* have normal karyotypes. (D) ICC analysis of *BBS1B* and c-*BBS1B* iPSC lines with pluripotency markers TRA-1-60 and *NANOG*. Scale bar, 50  $\mu$ m; (E) H&E staining of *BBS1B* and c-*BBS1B* iPSC-derived teratoma sections demonstrating cell types representing all three germ layers. Scale bar, 100  $\mu$ m.

**Figure S5. BBS mutations do not affect ciliogenesis in human fibroblasts.**

(A) Immunostaining of primary cilia in human fibroblasts. ACIII, ARL13B and  $\gamma$ -Tubulin are ciliary markers. Draq5 is used for nuclear staining. Scale bar, 20 $\mu$ m. (B-C) Quantification of percentage of ciliated cells (n=3 images per line) (B) and cilia length (n=15 cells) (C) in (A). (D) Immunostaining of primary cilia in human fibroblasts: Control 1, *BBS1A*, *BBS10A* and *BBS10B*. Acetylated tubulin (Ac-tub) and Pericentrin were used as ciliary markers. Scale bar: 5 $\mu$ m. (E) Quantification of cilia length in D (n=14 cells for each line). One-way ANOVA analysis was conducted. No significant differences were observed in (B), (C) or (E).

**Figure S6. BBS mutations do not affect efficiency of neuronal differentiation or electrophysiology of iPSC-derived Tuj1+ neurons.**

(A) Schematic of the neuronal differentiation protocol (modified from Chambers, SM et al, 2009 (35)). TGF- $\beta$  inhibitor--A83, a substitute for SB-431542, and BMP inhibitor LDN were used for dual inhibition. Day12 neuron progenitors (NPs) generated via dual SMAD inhibition

were passaged onto Poly-ornithine/Laminin (PO/LA)-coated plates in N2/A83/LDN medium. Neurons were obtained around day 30 by culturing the NPs on PO/LA plates in N2/B27/BDNF/DAPT medium. (B) Tuj1 staining of Day 34 iPSC-derived neurons from Control1, BBS1A, BBS1B, BBS10A and BBS10B lines. Scale bar, 200 $\mu$ m. (C) Percentage of NCAM+ cells from FACS analysis. (D) Bar graph showing the mRNA expression of MAP2 in iPSC-derived neurons from lines as indicated (N=2-5). (E) Whole cell patch clamp of control and BBS iPSC-derived neurons. Red trace indicates one action potential train after current stimulation.

**Figure S7. SHH/FGF8 increases cilia length in BBS10 iPSC-derived neurons.**

(A) SHH/FGF8 treatment increased cilia length in BBS10 iPSC-derived neurons. ACIII staining of primary cilia in Day 38 control and BBS iPSC-derived neurons. Day 35 iPSC-derived Tuj1+ neurons were treated with 0 or 100ng/ml SHH/FGF8 for 3 days. Neurons were fixed and stained with ACIII. The effect was most striking in BBS10 mutant neurons, in which “noodle-like” primary cilia were observed. Scale bar, 20 $\mu$ m. (B) Quantification of cilia length in (A). \*\*\*\*  $p < 0.0001$  by 2-way ANOVA analysis followed by Bonferroni’s multiple comparison test.

**Figure S8. Generation of transgenic Flag-BBS1/BBS10-GFP iPSC lines.**

(A) Schematic of the CD615-Ubc1-FLAG-BBS-GFP lentiviral plasmid construct. (B) Experimental flows for generating BBS transgenic iPSC lines using lentivirus made from plasmid in A. BBS iPSCs were infected with lentiviral particles. 48 hrs later, the virus-containing medium was removed and hygromycin (200ug/ml) selection was applied until stable Flag-BBS10-GFP cell lines were obtained. The upper right panel shows the expression of Flag-BBS10-GFP in the transgenic *BBS10A* iPSCs, as pointed out by arrows. (C) Western blot analysis to confirm the expression of Flag-BBS10-GFP in different BBS iPSC clones. GFP and BBS10 were probed. Arrow points out Flag-BBS10-GFP band. (D) Overexpression of *BBS10* in Flag-BBS10 transgenic BBS10A iPSC-derived neurons (n=3). \*\*  $p < 0.01$ , \*\*\*\*  $p < 0.0001$ , One-way ANOVA analysis followed Tukey’s multiple comparisons test.

**Figure S9. scRNA-seq of iPSC-derived hypothalamic neurons.**

(A) Heatmap of hierarchical clustering analysis across all 14 clusters for cluster marker gene identification. (B) Summary of ratios of TUBB3+, MAP2+, SST+ and POMC+ in all 14 clusters from *BBS1* and *c-BBS1* integration. Ratio per cluster = positive cells/total cells. Cut off: median expression level.

**Figure S10. Gene ontology analysis of differentially expressed genes in neuronal clusters.**

(A) Distribution of differentially expressed genes in all 14 clusters. No. of up- and down-regulated expressed genes (*BBS1B* vs *c-BBS1B*,  $P < 0.05$ ) were recorded. (B-G) Gene ontology for biological process analysis for clusters 1, 4, 7-10. Adjusted p-value was used for this plot.

**Figure S11. KEGG pathway analysis of differentially expressed genes in neuronal clusters.**

KEGG pathway analysis of both up- and down-regulated differentially expressed genes (*BBS1B* vs *c-BBS1B*) for clusters 1, 3, 7-10. Adjusted p-values were used for this plot.

**Figure S12. scRNA-seq reveals that *BBS1M390R* mutation decreases expression of genes related to type II diabetes mellitus pathway and Wnt pathways.**

Heatmap of genes involved in type II diabetes mellitus (A) and Wnt signaling (B) from KEGG pathway analysis. Clusters 1, 3, 4, 7 and 9 of BBS1B and c-BBS1B iPSC-derived hypothalamic neurons ( $p < 0.05$ ) were included.

**Figure S13. Wnt and SHH signaling molecule expression from RNA-seq of iPSC-derived hypothalamic neurons.** The expression of FZD1(A), AXIN2 (B), GLI1(C) and PTCH1(D) from RNA-seq analysis of Day45 Control and BBS iPSC-derived hypothalamic neurons. Gene expression was normalized to TBP ( $n=1$ ).

**Figure S14. Knockdown of *BBS10* in control iPSCs using lentiviral shRNA.**

Control iPSCs were infected with control and two *BBS10* lentiviral shRNAs for 48hrs. These iPSC were further treated with  $1\mu\text{g/ml}$  puromycin selection until puromycin resistant iPSC were obtained. Expression of *BBS10* in shRNA knockdown iPSC lines were determined by RT-qPCR ( $n=2$ ).

**Figure S15. BBS mutations impair leptin signaling in RFP-LEPR transgenic human fibroblasts.**

(A) Western blot analysis of leptin signaling in human control, BBS and JBST fibroblasts. Human fibroblasts were serum starved overnight and exposed to 0, 0.2 and  $2\mu\text{g/ml}$  leptin for 30min. (B) Quantification of p-STAT3/STAT3 from A ( $n=1$ ). (C) Diagram of the lentiviral RFP-LEPR construct. (D) Live cell imaging shows RFP expression in RFP-LEPR transgenic control and BBS fibroblast lines as indicated. Scale bar:  $100\mu\text{m}$ ; (E) Western blot analysis of leptin signaling in RFP-LEPR transgenic human fibroblasts. Control, BBS1B and BBS10A RFP-LEPR transgenic fibroblasts were included. Cells were exposed to 0, 0.1 and  $1\mu\text{g/ml}$  leptin for 30min. p-STAT3, STAT3 and ACTIN were analyzed from cell lysates. (F) Quantification of p-STAT3/STAT3 from WB was shown on the right ( $n=1$ ). (G) Staining of p-STAT3 in control and BBS RFP-LEPR transgenic human fibroblasts. Human fibroblasts were fasted overnight and exposed to  $1\mu\text{g/ml}$  leptin for 30min. Cells were fixed and stained with p-STAT3 and Hoechst. Scale bar,  $200\mu\text{m}$ .

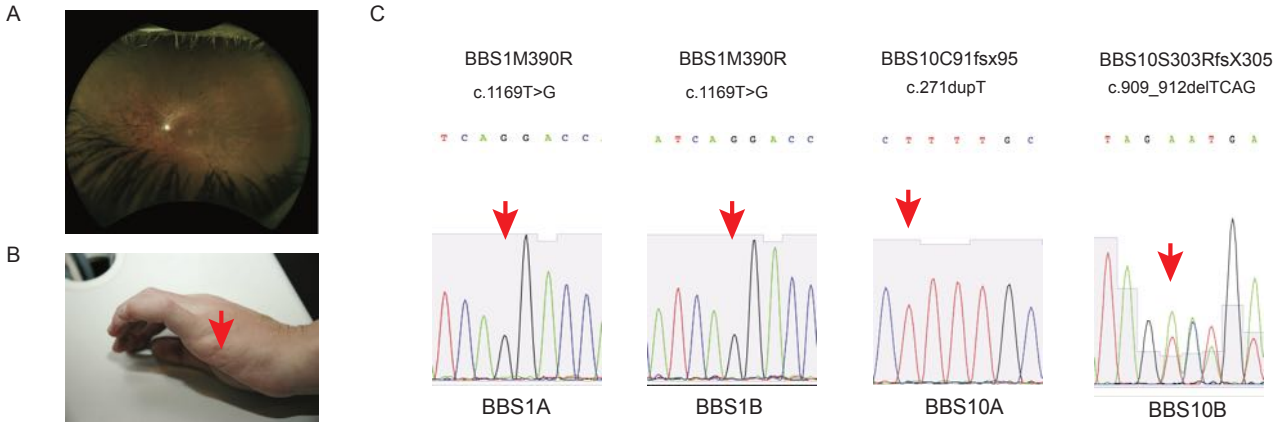


**Figure S1. BBS patients - phenotype and genotype.**

(A-B) Clinical phenotypes of BBS subject BBS1B includes obesity, retinitis pigmentosa (A), polydactyly (B), cognitive impairment and renal cysts. Arrow points to the scar after surgery to remove the extra digit. (C) Dideoxy-sequencing confirming the mutations identified by genetic testing or genome sequencing in four BBS subjects. Red arrows indicate mutation sites.

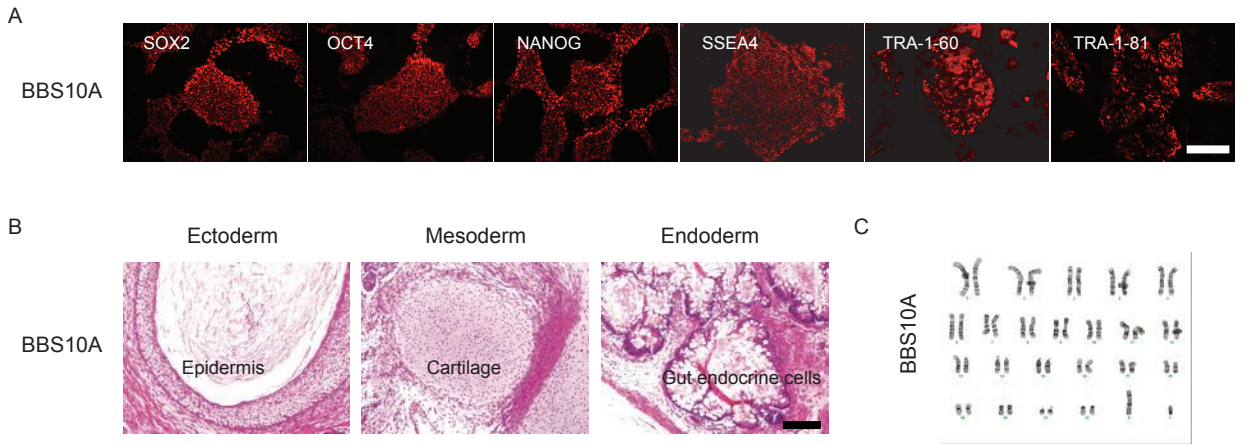
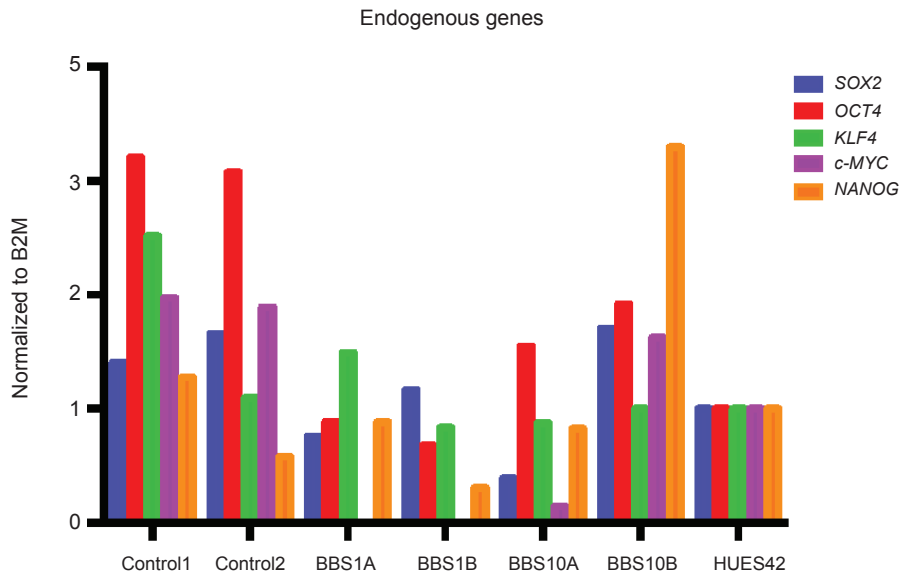


**Figure S2. *BBS10A* iPSC line is pluripotent and has a normal karyotype.**

(A) Immunocytochemistry analysis of *BBS10A* iPSC line with pluripotency markers as indicated. Scale bar, 200 $\mu$ m; (B) H&E staining of *BBS10A* iPSC-derived teratoma sections. Cell types representing all three germ layers in iPSC-derived teratoma were identified. Scale bar, 200 $\mu$ m. (C) *BBS10A* iPSC had a normal karyotype.

A



B

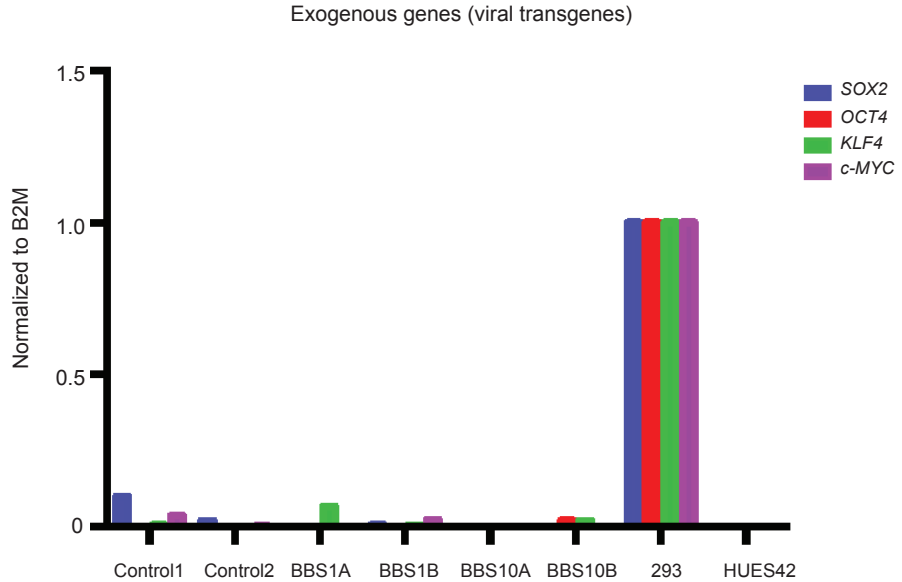
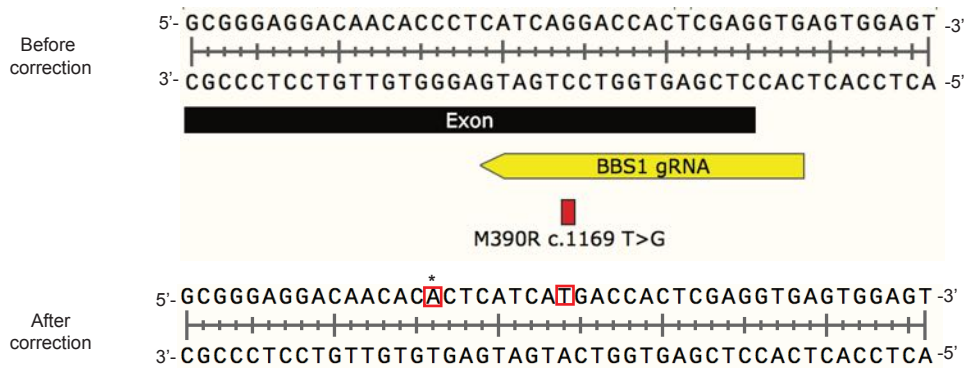


**Figure S3. Reprogramming re-activates endogenous pluripotency genes and silences exogenous genes in iPSCs.**

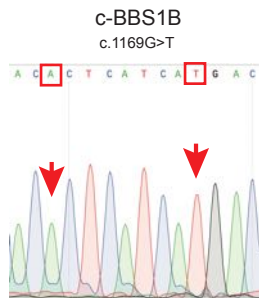
(A) Expression of endogenous stem cell markers: *SOX2*, *OCT4*, *KLF4*, *c-MYC* and *NANOG* in indicated iPSC lines (passage 8-10)(n=1). Human embryonic stem cell line HUES42 was used as a positive control for endogenous stem cell gene expression; (B) Expression of retroviral genes in reprogrammed iPSC as indicated. 293 cells transduced with retroviral cocktail for 48 hours were used as a positive control for viral gene expression. HUES42 was used as a negative control (n=1).

A

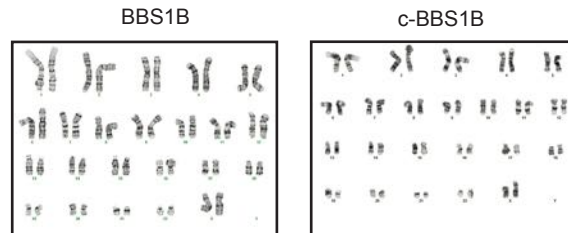
BBS1 gRNA: 5'-CACCTCGAGTGGTCTGATG-3' PAM motif: AGG



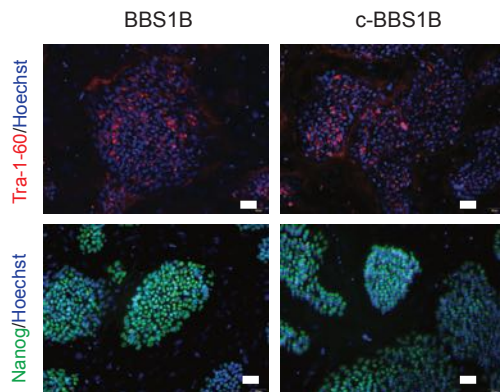
B



C



D



E

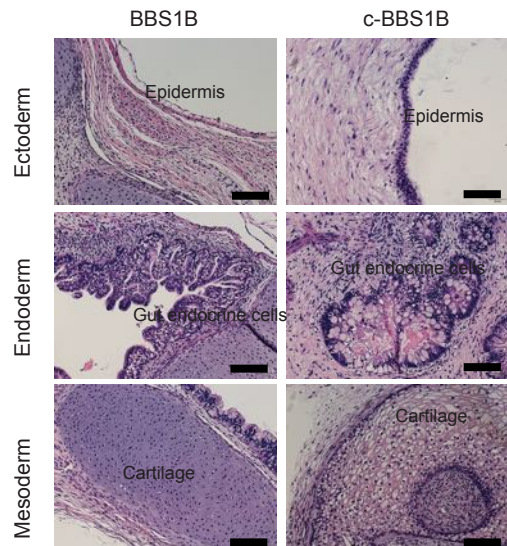


### Figure S4. Generation of isogenic control iPSC line (*c-BBS1B*) using CRISPR/Cas9.

(A) Schematic of targeting the *BBS1* locus. Sequence of genomic DNA around the mutation site in *BBS1M390R* before (top) and after (bottom) CRISPR-Cas9 correction. Sequence of guide RNA (gRNA) for *BBS1 M390R* indicated in yellow. Red rectangle marks the mutation. Star marks the silent mutation introduced to avoid cutting of the repair oligo. (B) Sanger sequencing after TOPO cloning confirmed the homozygous correction of *BBS1M390R* mutation in the isogenic control line referred to as *c-BBS1B*. (C) *BBS1B* and *c-BBS1B* have normal karyotypes. (D) ICC analysis of *BBS1B* and *c-BBS1B* iPSC lines with pluripotency markers TRA-1-60 and NANOG. Scale bar, 50  $\mu$ m; (E) H&E staining of *BBS1B* and *c-BBS1B* iPSC-derived teratoma sections demonstrating cell types representing all three germ layers. Scale bar, 100  $\mu$ m.

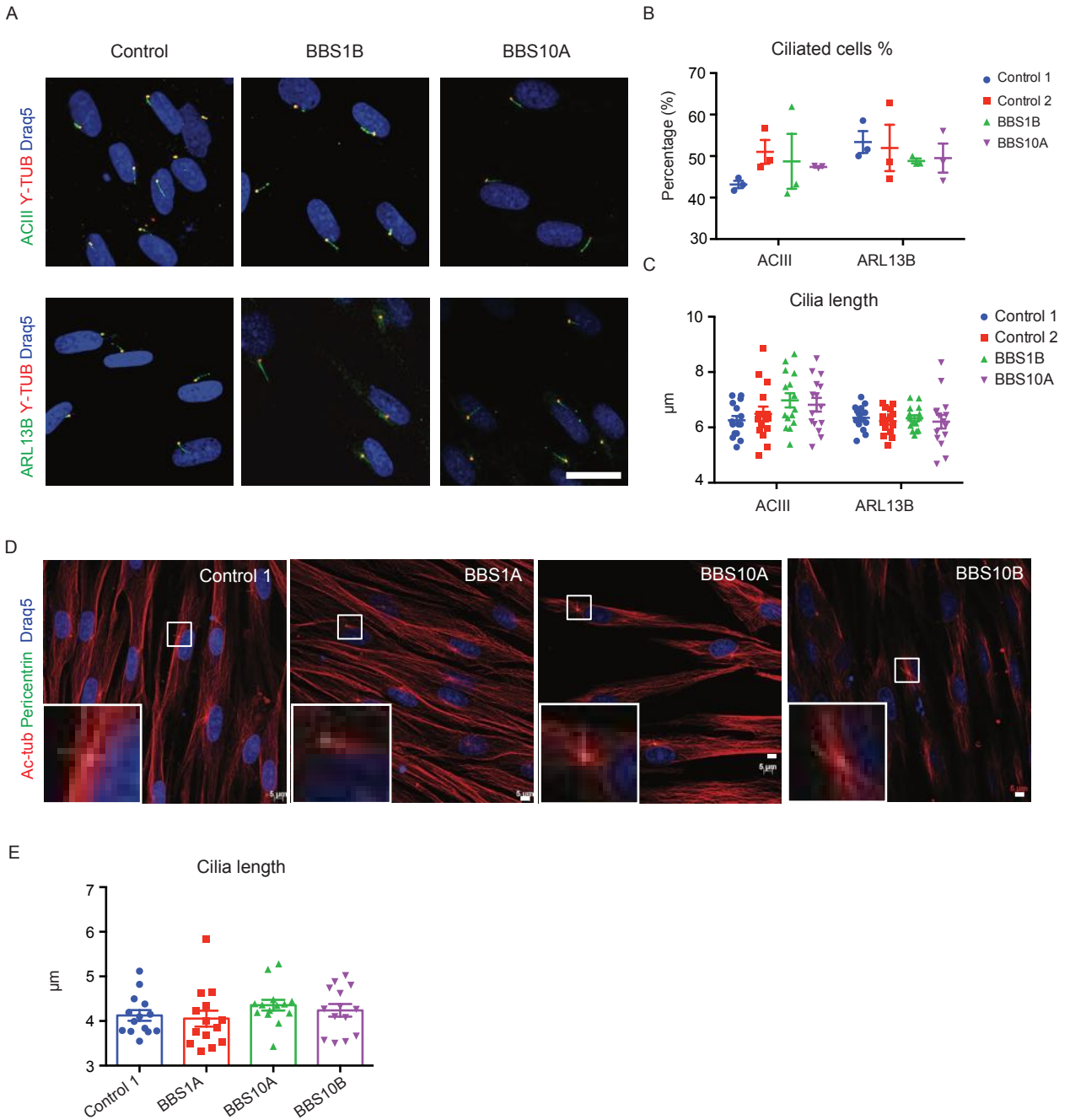


**Figure S5. BBS mutations do not affect ciliogenesis in human fibroblasts.**

(A) Immunostaining of primary cilia in human fibroblasts. ACIII, ARL13B and Y-Tubulin are ciliary markers. Draq5 is used for nuclear staining. Scale bar, 20 $\mu$ m. (B-C) Quantification of percentage of ciliated cells (n=3 images per line) (B) and cilia length (n=15 cells) (C) in (A). (D) Immunostaining of primary cilia in human fibroblasts: Control 1, BBS1A, BBS10A and BBS10B. Acetylated tubulin (Ac-tub) and Pericentrin were used as ciliary markers. Scale bar: 5 $\mu$ m. (E) Quantification of cilia length in D (n=14 cells for each line). One-way ANOVA analysis was conducted. No significant differences were observed in (B), (C) or (E).

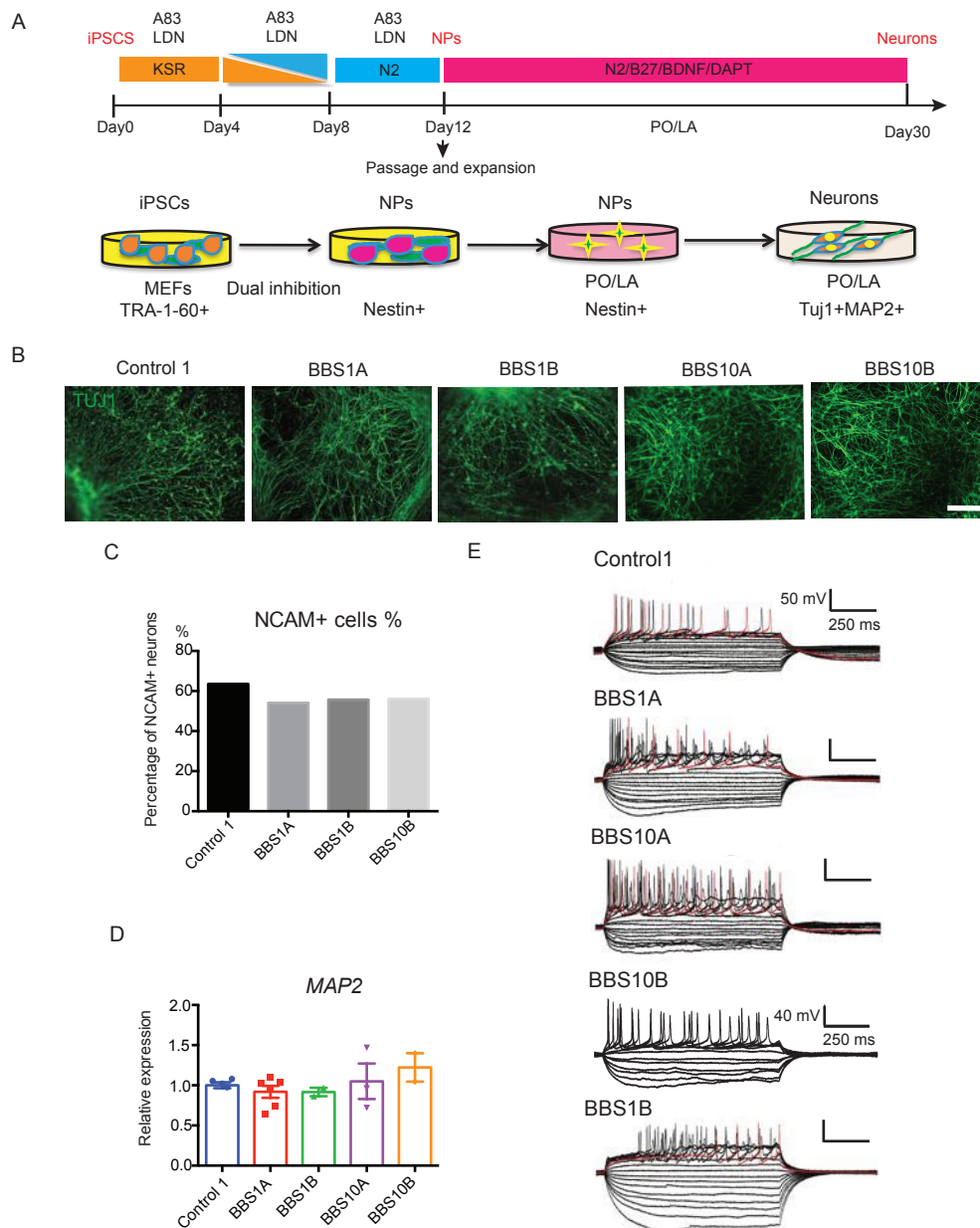
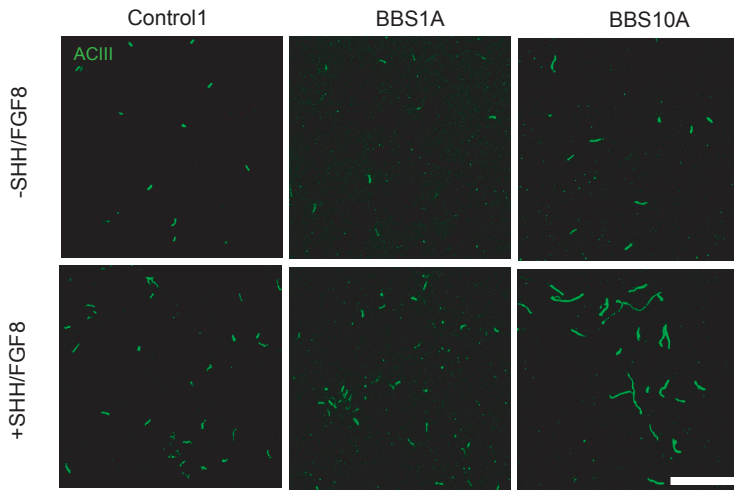


**Figure S6. BBS mutations do not affect efficiency of neuronal differentiation or electrophysiology of iPSC-derived TUJ1+ neurons.**

(A) Schematic of the neuronal differentiation protocol (modified from Chambers, SM et al, 2009 (35)). TGF- $\beta$  inhibitor--A83, a substitute for SB-431542, and BMP inhibitor LDN were used for dual inhibition. Day12 neuron progenitors (NPs) generated via dual SMAD inhibition were passaged onto Poly-ornithine/Laminin (PO/LA)-coated plates in N2/A83/LDN medium. Neurons were obtained around day 30 by culturing the NPs on PO/LA plates in N2/B27/BDNF/DAPT medium. (B) TUJ1 staining of Day 34 iPSC-derived neurons from control1, BBS1A, BBS1B, BBS10A and BBS10B lines. Scale bar, 200 $\mu$ m. (C) Bar graph showing the percentage of NCAM+ cells from FACS analysis. (D) Bar graph showing the mRNA expression of MAP2 in iPSC-derived neurons from lines as indicated (n=2-5). (E) Whole cell patch clamp of control and BBS iPSC-derived neurons. Red trace indicates one action potential train after current stimulation.

A



B

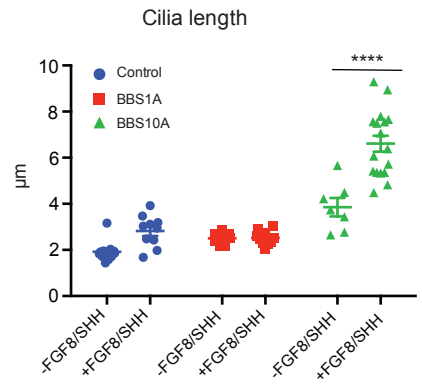


**Figure S7. SHH/FGF8 increases cilia length in *BBS10* mutant iPSC-derived neurons.**

(A) SHH/FGF8 treatment increased cilia length in *BBS10* iPSC-derived neurons. ACIII staining of primary cilia in Day 38 control and BBS iPSC-derived neurons. Day 35 iPSC-derived Tuj1+ neurons were treated with 0 or 100 ng/ml SHH/FGF8 for 3 days. Neurons were fixed and stained with ACIII. The effect was most striking in *BBS10* mutant neurons, in which “noodle-like” primary cilia were observed. Scale bar, 20µm. (B) Quantification of cilia length in (A). \*\*\*\*  $p < 0.0001$  by 2-way ANOVA analysis followed by Bonferroni’s multiple comparison test.

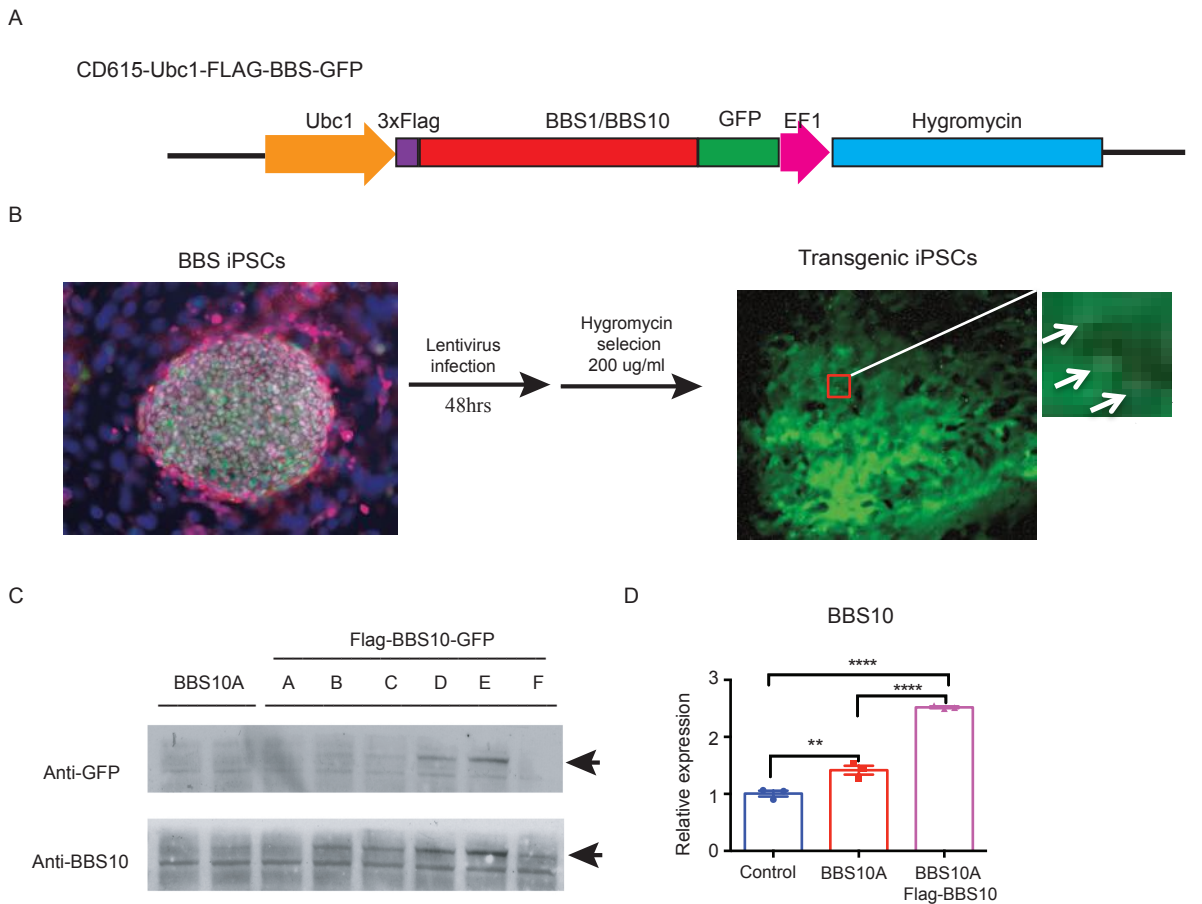
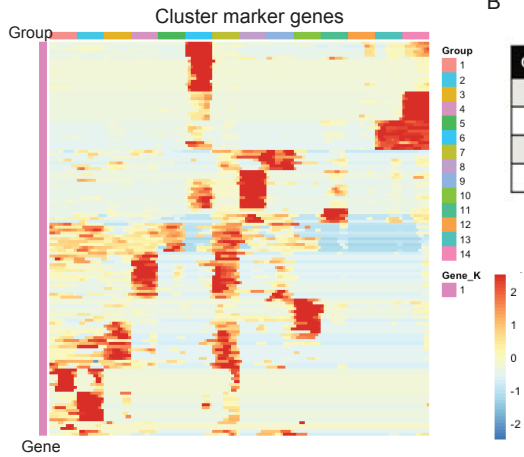


**Figure S8. Generation of transgenic Flag-BBS1/BBS10-GFP iPSC lines.**

(A) Schematic of the CD615-Ubc1-FLAG-BBS-GFP lentiviral plasmid construct. (B) Experimental flows for generating BBS transgenic iPSC lines using lentivirus made from plasmid in A. BBS iPSCs were infected with lentiviral particles. 48 hrs later, the virus-containing medium was removed and hygromycin (200ug/ml) selection was applied until stable Flag-BBS10-GFP cell lines were obtained. The upper right panel shows the expression of Flag-BBS10-GFP in the transgenic *BBS10A* iPSCs, as pointed out by arrows. (C) Western blot analysis to confirm the expression of Flag-BBS10-GFP in different BBS iPSC clones. GFP and BBS10 were probed. Arrow points out Flag-BBS10-GFP band. (D) Overexpression of *BBS10* in Flag-BBS10 transgenic *BBS10A* iPSC-derived neurons (n=3). \*\* p<0.01, \*\*\*\* p<0.0001, One-way ANOVA analysis followed Tukey's multiple comparisons test.

A



B

Cluster (ratio)	1	2	3	4	5	6	7	8	9	10	11	12	13	14
<b>TUBB3+</b>	0.67	0.58	0.51	0.52	0.03	0.08	0.72	0.28	0.38	0.59	0.21	0.02	0.06	0.11
<b>MAP2+</b>	0.72	0.64	0.87	0.38	0.19	0.04	0.78	0.79	0.77	0.50	0.73	0.27	0.39	0.31
<b>SST+</b>	0.43	0.20	0.42	0.98	0.62	0.07	0.91	0.11	0.33	0.06	0.44	0.54	0.40	0.35
<b>POMC+</b>	0.21	0.20	0.93	0.06	0.20	0.10	0.56	0.01	0.11	0.91	0.03	0.15	0.13	0.13

### Figure S9. scRNA-seq of iPSC-derived hypothalamic neurons.

(A) Heatmap of hierarchical clustering analysis across all 14 clusters for cluster marker gene identification. (B) Summary of ratios of TUBB3+, MAP2+, SST+ and POMC+ in all 14 clusters from *BBS1B* and *c-BBS1B* integration. Ratio per cluster = positive cells/total cells. Cut off: median expression level.

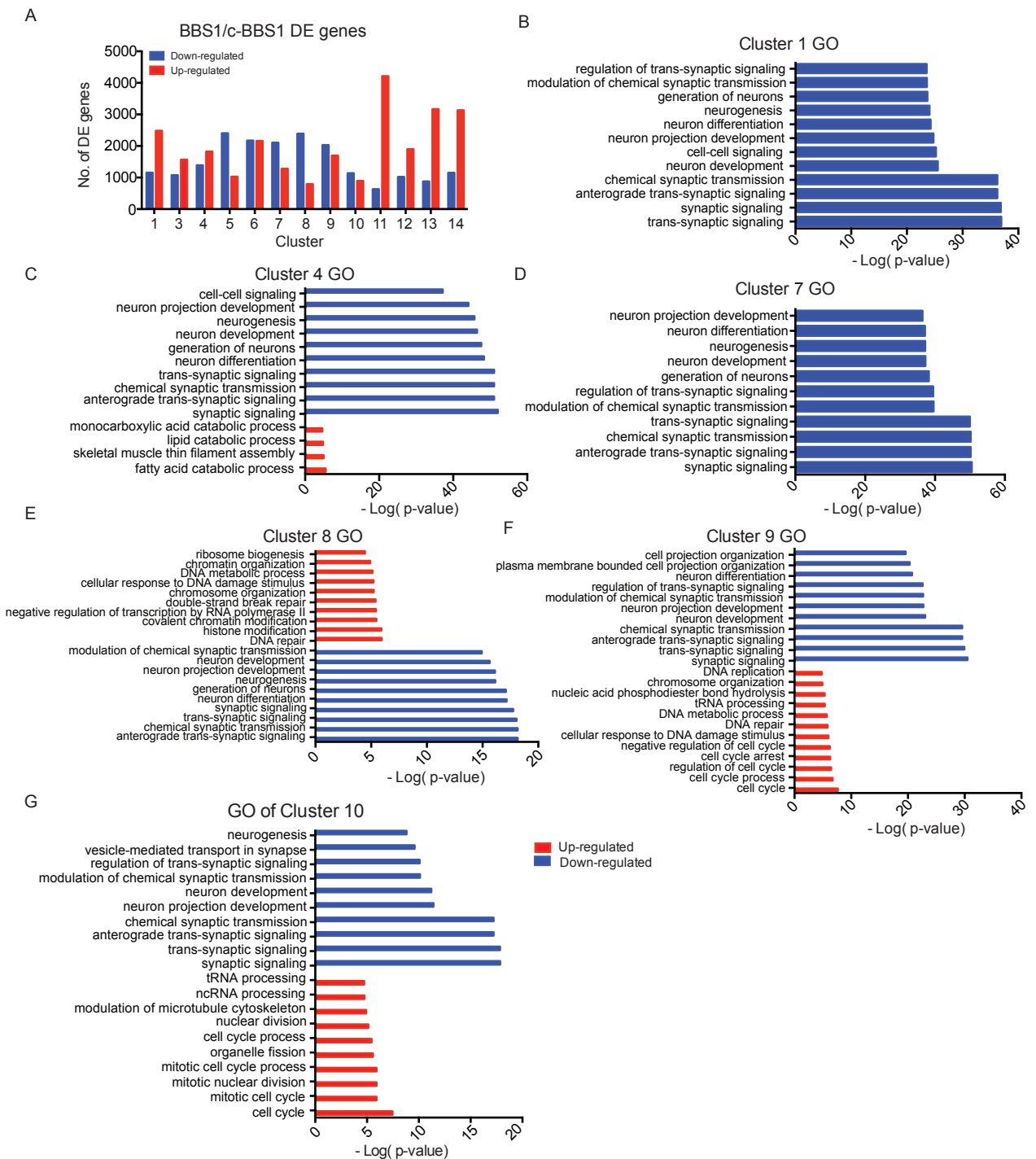


**Figure S10. Gene ontology analysis of differentially expressed genes in neuronal clusters.**

(A) Distribution of differentially expressed genes in all 14 clusters. No. of up- and down-regulated expressed genes (*BBS1B* vs *c-BBS1B*,  $P < 0.05$ ) were recorded. (B-G) Gene ontology for biological process analysis for clusters 1, 4, 7-10. Adjusted p-value was used for this plot.

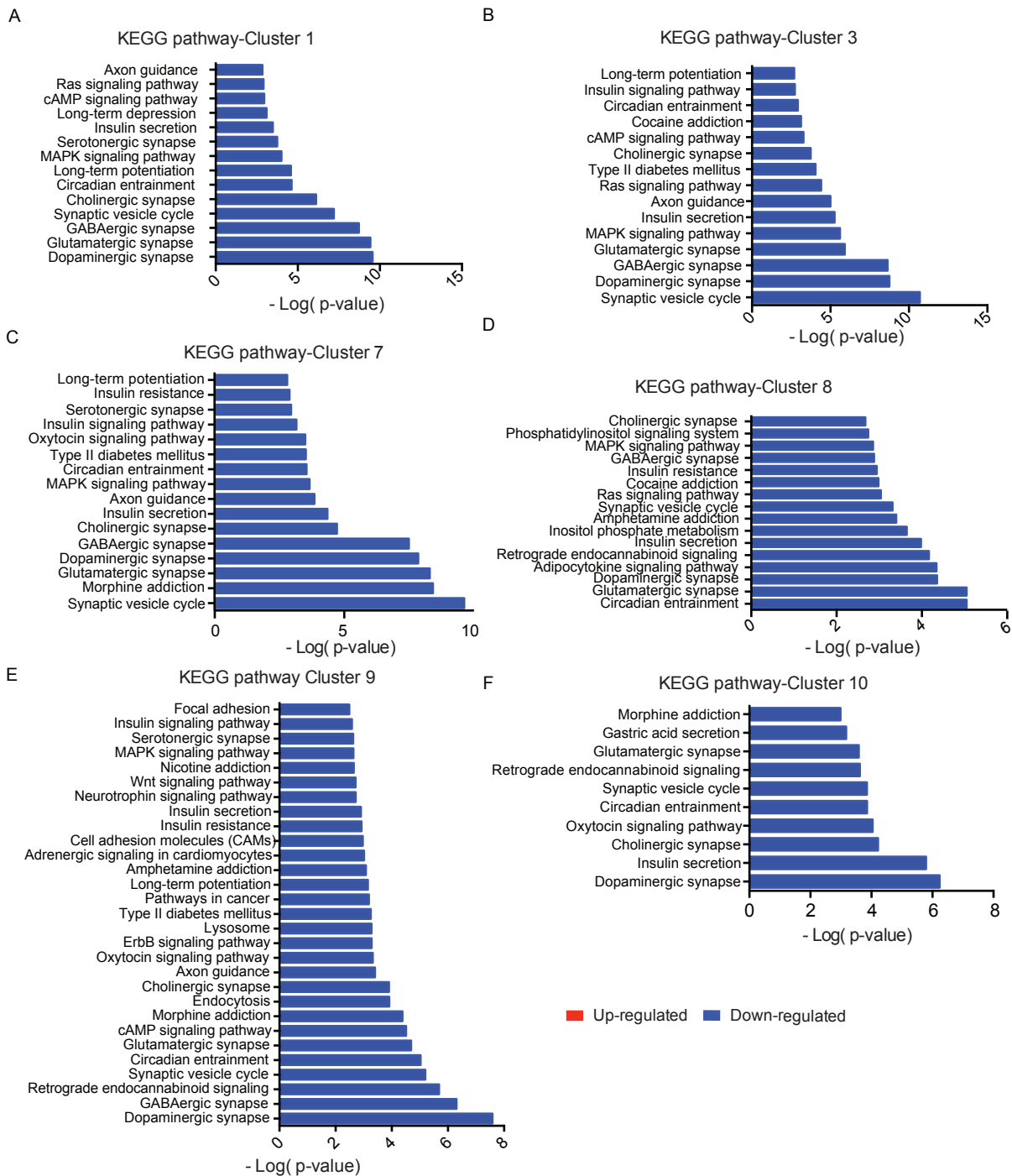
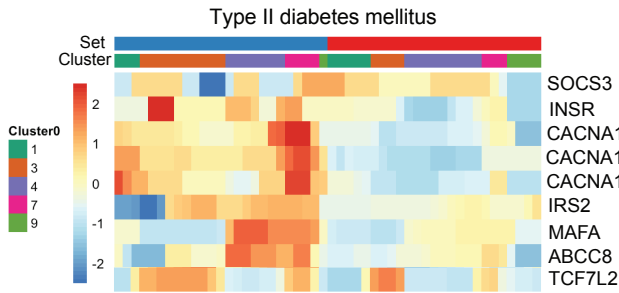


**Figure S11. KEGG pathway analysis of differentially expressed genes in neuronal clusters.** KEGG pathway analysis of both up- and down-regulated differentially expressed genes (*BBS1B* vs *c-BBS1B*) for clusters 1, 3, 7-10. Adjusted p-values were used for this plot.

A



B

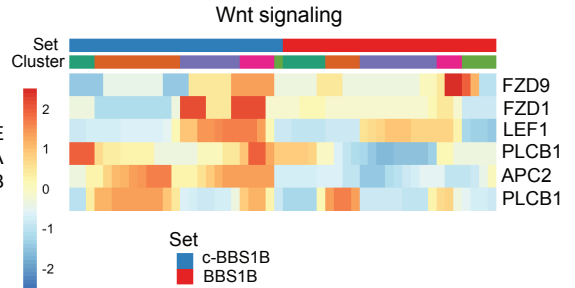


**Figure S12. scRNA-seq reveals that *BBS1M390R* mutation decreases expression of genes related to type II diabetes mellitus and Wnt pathways.**

Heatmap of genes involved in type II diabetes mellitus (A) and Wnt signaling (B) from KEGG pathway analysis. Clusters 1, 3, 4, 7 and 9 of *BBS1B* and *c-BBS1B* iPSC-derived hypothalamic neurons ( $p < 0.05$ ) were included.

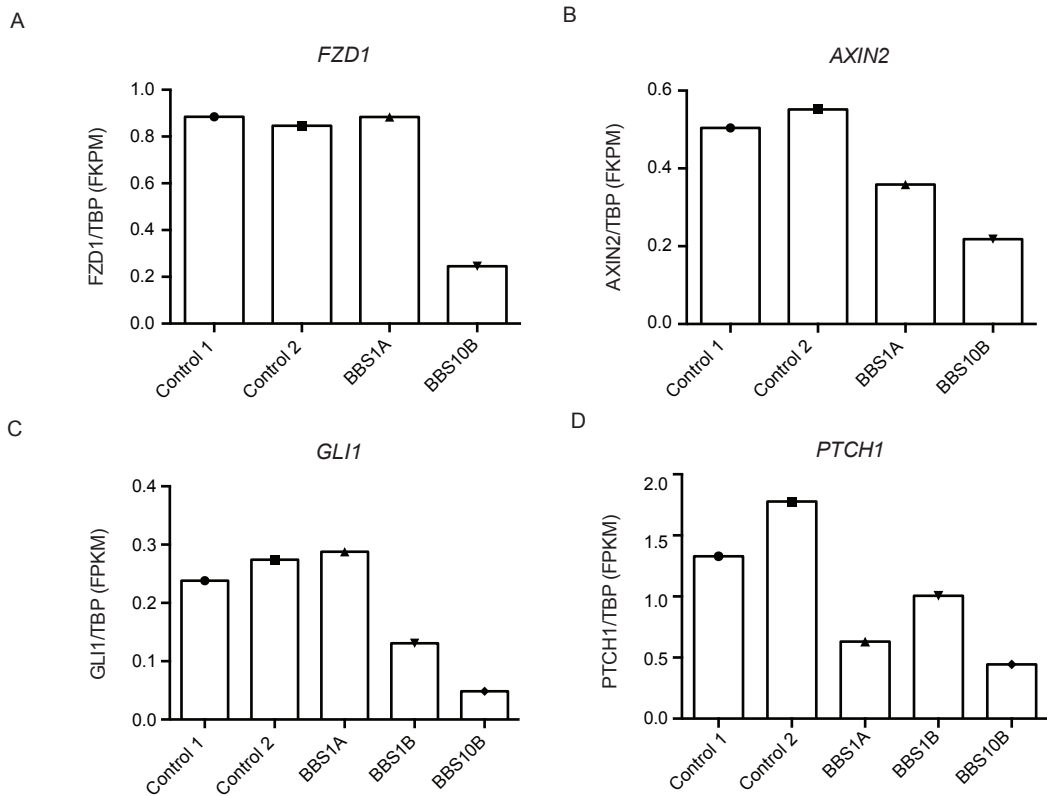


**Figure S13. Wnt and SHH signaling molecule expression from RNA-seq of iPSC-derived hypothalamic neurons.** The expression of *FZD1*(A), *AXIN2* (B), *GLI1*(C) and *PTCH1*(D) from RNA-seq analysis of Day45 Control and BBS iPSC-derived hypothalamic neurons. Gene expression was normalized to TBP (n=1).

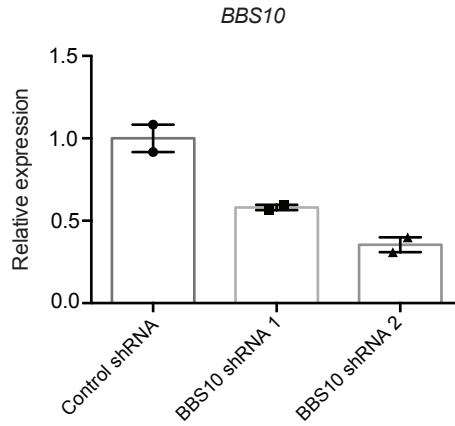


**Figure S14. Knockdown of *BBS10* in control iPSCs using lentiviral shRNA.**

Control iPSCs were infected with control and two *BBS10* lentiviral shRNAs for 48hrs. These iPSC were further treated with  $1\mu\text{g/ml}$  puromycin selection until puromycin resistant iPSC were obtained. Expression of *BBS10* in shRNA knockdown iPSC lines were determined by QPCR (n=2).

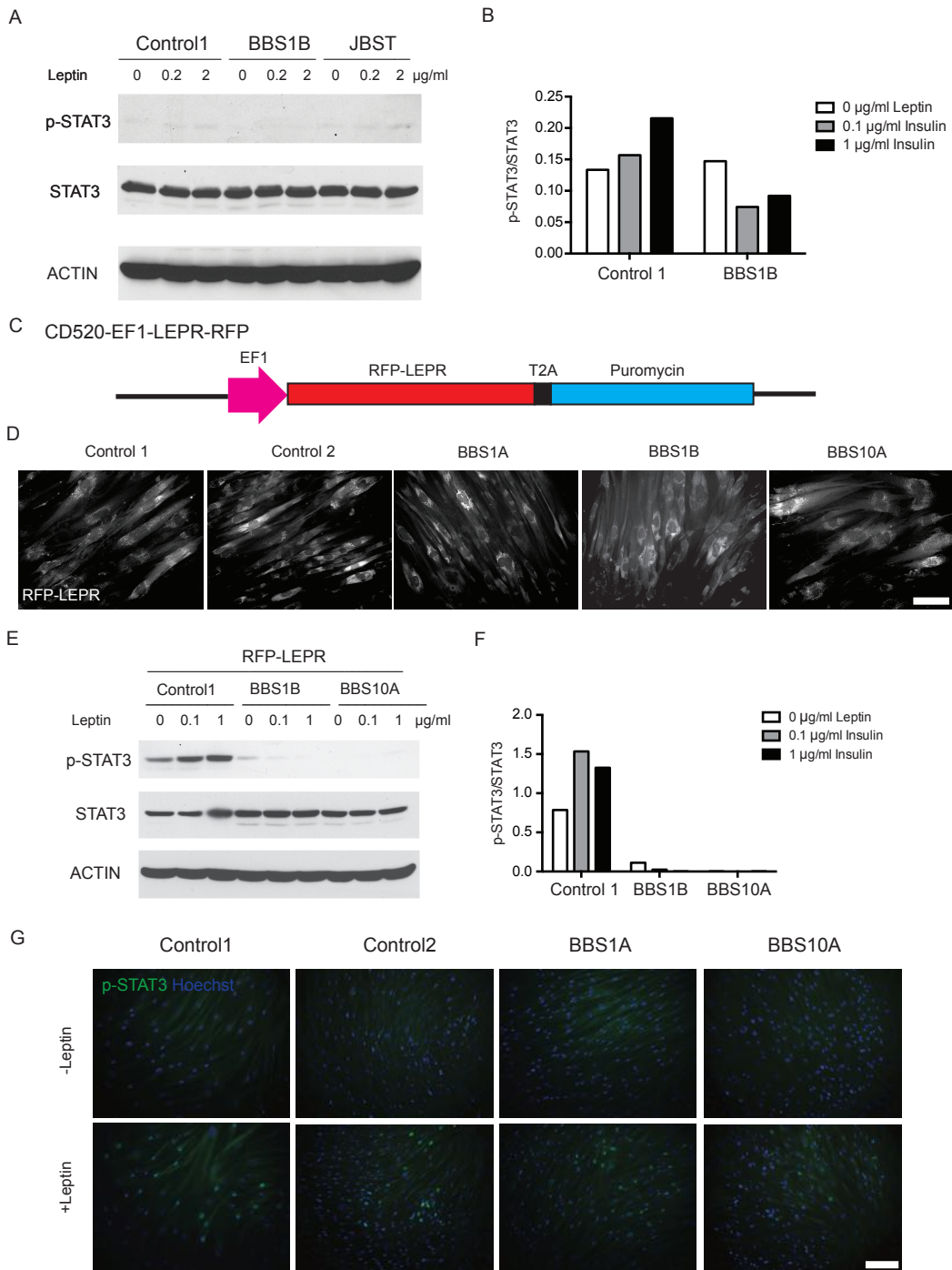


**Figure S15. BBS mutations impair leptin signaling in RFP-LEPR transgenic human fibroblasts.**

(A) Western blot analysis of leptin signaling in human control, BBS and JBST fibroblasts. Human fibroblasts were serum starved overnight and exposed to 0, 0.2 and 2 µg/ml leptin for 30min. (B) Quantification of p-STAT3/STAT3 from A (n=1). (C) Diagram of the lentiviral RFP-LEPR construct. (D) Live cell imaging shows RFP expression in RFP-LEPR transgenic control and BBS fibroblast lines as indicated. Scale bar: 100 µm; (E) Western blot analysis of leptin signaling in RFP-LEPR transgenic human fibroblasts. Control, BBS1B and BBS10A RFP-LEPR transgenic fibroblasts were included. Cells were exposed to 0, 0.1 and 1 µg/ml leptin for 30min. p-STAT3, STAT3 and ACTIN were analyzed from cell lysates. (F) Quantification of p-STAT3/STAT3 from WB was shown on the right (n=1). (G) Staining of p-STAT3 in control and BBS RFP-LEPR transgenic human fibroblasts. Human fibroblasts were fasted overnight and exposed to 1 µg/ml leptin for 30min. Cells were fixed and stained with p-STAT3 and Hoechst. Scale bar, 200µm.

**Table S1. Summary of BBS primary fibroblast and iPSC lines.**

ID	Diagnosis	Affected	Source	Genotyping	Age	Sex	iPSC Line
GM05948	BBS	Yes	Coriell	BBS10 C91fsX95/C91fsX95	18 YR	Male	<b>BBS10A</b>
GM05950	BBS	Yes	Coriell	BBS10 S303RfsX305/+	19 YR	Male	<b>BBS10B*</b>
1085	BBS	Yes	Skin Biopsy	BBS1 M390R/M390R	29 YR	Male	<b>BBS1A*</b>
1097	BBS	Yes	Skin Biopsy	BBS1 M390R/M390R	45 YR	Female	<b>BBS1B*</b>
1016	Control	No	Skin Biopsy	Normal	34 YR	Male	<b>Control1*</b>
1023	Control	No	Skin Biopsy	Normal	25 YR	Male	<b>Control2*</b>
1097 CRISPR line	Isogenic control						<b>c-BBS1B</b>
1065	BBS	Yes	Skin Biopsy	BBS6 L363P/L363P	18 YR	Male	Fibroblast and iPSC
1084	BBS	Yes	Skin Biopsy	ND	5 YR	Male	Fibroblast and iPSC
1100	BBS	Yes	Skin Biopsy	BBS13 <sup>R479H/+</sup>	7 YR	Female	Fibroblast
1122	BBS	Yes	Skin Biopsy	ND	27YR	Male	Fibroblast
1198	BBS	Yes	Skin Biopsy	ND	30YR	Female	Fibroblast
1199	BBS	Yes	Skin Biopsy	ND	35YR	Male	Fibroblast

\*As reported in previous published paper (Wang et al., 2015).

**Table S2. Primers for genotyping.**

<b>Gene</b>	<b>Forward Primer</b>	<b>Reverse Primer</b>
BBS1M390R	AGGGCCAGTGATATTTGGTCTGGA	TGTAGGCCTTACTTTCCACACCCA
BBS10c91fsX 95	TTAAGATGTGGGAAGCCAGCCTTCTG	TGAAACGTTAGGAGAGCCTGGG
BBS10S303Rf sX305	CAGGATCATAGCTGGTCTTGTGCT	AAAGGCCTGTGGTGGTACAAATGG

**Table S3. qPCR primers.**

<b>Gene</b>	<b>Forward Primer</b>	<b>Reverse Primer</b>
<i>NANOG</i>	ACAACTGGCCGAAGAATAGCA	GGTTCCCAGTCGGGTTCAC
<i>BBS10</i>	CCTGGAGGCGCTACACTTAG	CAATTTTTCCAATGCCTTCC
<i>ADCY3</i>	CGCACAGGTAGAGGAAGACG	ATCATCTCCGTGGTCTCCTG
<i>IFT88</i>	GGTCCAAGACATCTCTGGCATCATCA	AAATGCAGAGCCTCTCAAAGCTGC
<i>ARL13B</i>	GAACCAGTGGTCTGGCTGAGTT	GTTTCAGGTGGCAGCCATCACT
<i>PATCHED1</i>	TTCTTGTTGTGGGCCTCCTCATA	CTCTTCTCCAATCTTCTGGCGAGT
<i>GLII</i>	ACAGTCCTTCTGTCCCCACA	CCAGCGCCCAGACAGAG
<i>FZD1</i>	CAGCACAGCACTGACCAAAT	TCAACTACCACTTCCTGGGG
<i>AXIN2</i>	ACAGGATCGCTCCTCTTGAA	AAGTGCAAACCTTCGCCAAC
<i>LEPR</i>	ATGTTCCGAACCCCAAGAAT	GGACCACATGTCAGTATGC
<i>SOCS3</i>	GAGCCAGCGTGGATCTG	GGCTCAGCCCCAAGGAC
<i>TBP</i>	AACAACAGCCTGCCACCTTA	GCCATAAGGCATCATTGGAC
<i>B2M</i>	TAGCTGTGCTCGGGCTACT	TCTCTGCTGGATGACGCG
<i>Pomc</i> (mouse)	CCATAGATGTGTGGAGCTGGTG	CATCTCCGTTGCCAGGAAACAC
<i>Npy</i> (mouse)	TACTCCGCTCTGCGACACTACA	GGCGTTTTCTGTGCTTTCCTTCA
<i>Tbp</i> (mouse)	CTACCGTGAATCTTGGCTGTAAAC	AATCAACGCAGTTGTCCGTGGC

**Table S4. List of antibodies.**

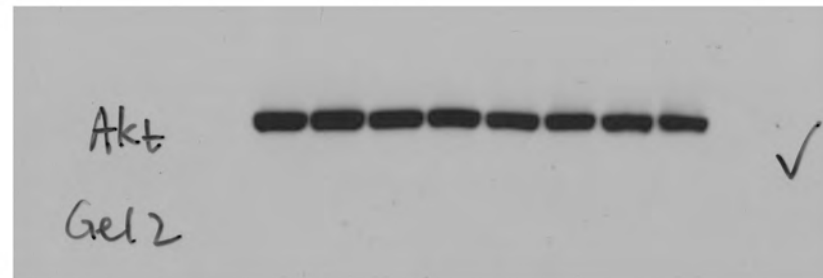
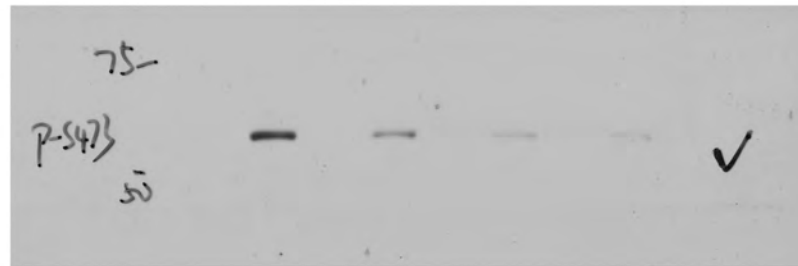
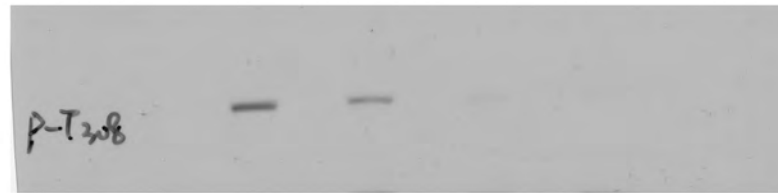
<b>Antibody</b>	<b>Species</b>	<b>Dilution</b>	<b>Source</b>	<b>Catalog No.</b>
TRA-1-60	Mouse	1:300	Millipore	MAB4360
TRA-1-81	Mouse	1:300	Millipore	MAB4381
NANOG	Goat	1:500	R&D Systems	AF1997
SOX2	Rabbit	1:500	Stemgent	09-0024
OCT4	Rabbit	1:500	Stemgent	09-0023
SSEA4	Mouse	1:300	R&D Systems	MAB1435
TUJ1	Rabbit	1:500	Sigma	T2200
TUJ1	Mouse	1:500	Sigma	T5076
MAP2	Chicken	1:10,000	Abcam	AB5392
ACIII	Rabbit	1:100	Santa Cruz	sc-588
ARL13B	Rabbit	1:1000	Gift from Tamara Caspary (Caspary et al., 2007)	
Gamma-Tubulin	Mouse	1:500	Sigma	T6557
Acetylated-tubulin	Mouse	1:500	Sigma	T6793
Smoothened	Rabbit	1:500	Gift from Kathryn Anderson, NYC	
FLAG	Mouse	WB 1:500	Sigma	F1804
Myc	Mouse	WB 1:500	Cell signaling	2276
p-IR $\beta$	Rabbit	WB 1:500	Cell signaling	3024
IR $\beta$	Rabbit	WB 1:1000	Cell signaling	3025
RFP	Rabbit	WB 1:500	Abcam	AB62341
$\alpha$ MSH	Sheep	1:1000	Millipore	AB5087
Beta-endorphin	Rabbit	1:500 and RIA	Antibodyregistry.org	AB_2756516
$\alpha$ MSH	Rabbit	RIA	Antibodyregistry.org	AB_2756515
POMC	Mouse	ELISA	Antibodyregistry.org	AB_2756529 AB_2756530
AGRP	Goat	1:500	Neuromics	GT15023
Neurofilament H	Chicken	1:1000	Millipore	AB5539
p-STAT3	Mouse	1:200 WB1:1000	Cell signaling	4113
p-STAT3	Rabbit	1:200 WB 1:1000	Cell signaling	9145
p-AKT(T308)	Rabbit	WB 1:1000	Cell signaling	9275
p-AKT(S473)	Rabbit	WB 1:1000	Cell signaling	4060
STAT3	Rabbit	WB 1:1000	Cell signaling	12640
AKT	Rabbit	WB 1:1000	Cell signaling	9272
Actin	Rabbit	WB 1:1000	Cell signaling	8457

## **Bibliography**

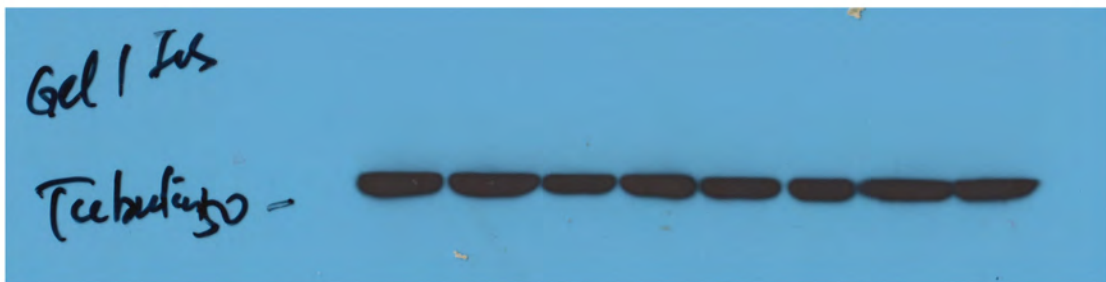
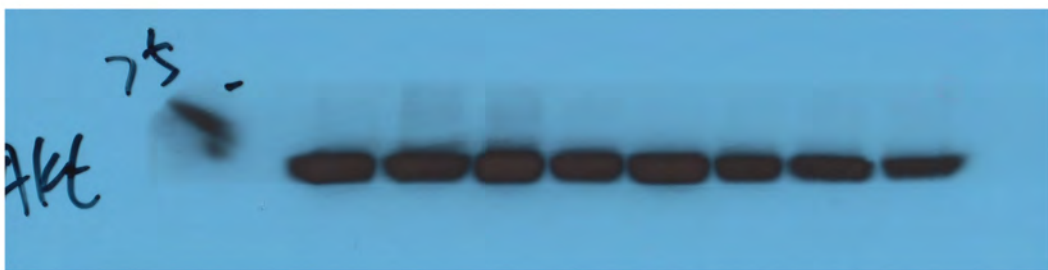
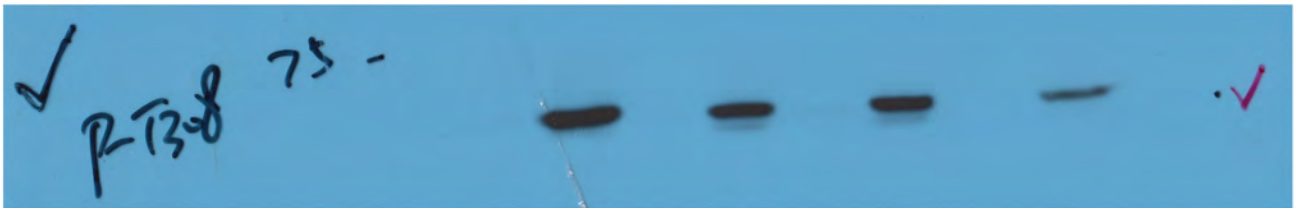
Caspary, T., Larkins, C.E., and Anderson, K.V. (2007). The graded response to Sonic Hedgehog depends on cilia architecture. *Dev Cell* 12, 767-778.

Wang, L., Meece, K., Williams, D.J., Lo, K.A., Zimmer, M., Heinrich, G., Martin Carli, J., Leduc, C.A., Sun, L., Zeltser, L.M., *et al.* (2015). Differentiation of hypothalamic-like neurons from human pluripotent stem cells. *J Clin Invest* 125, 796-808.

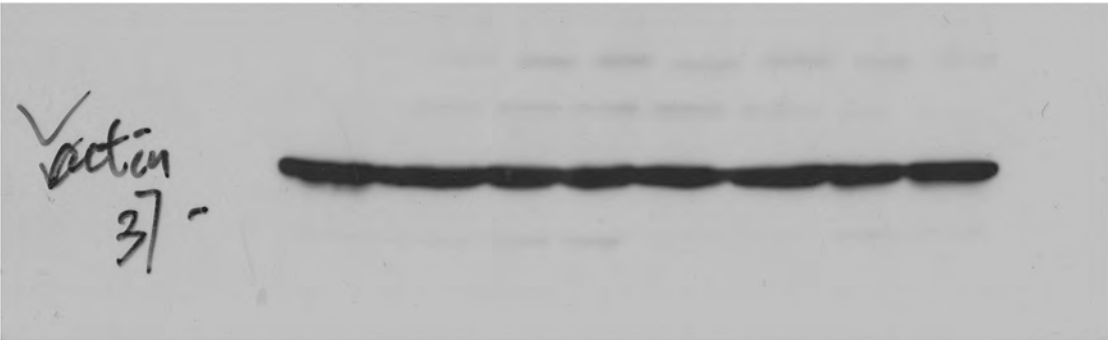
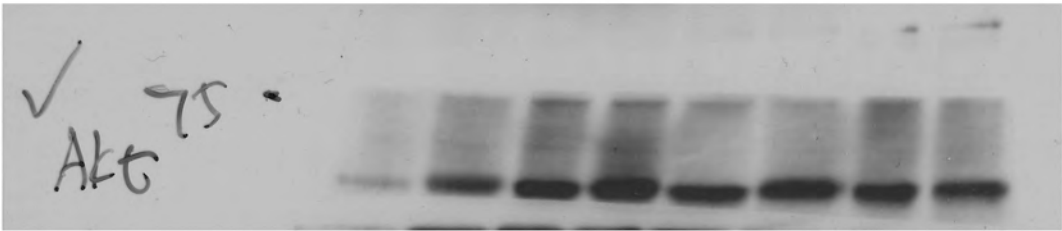
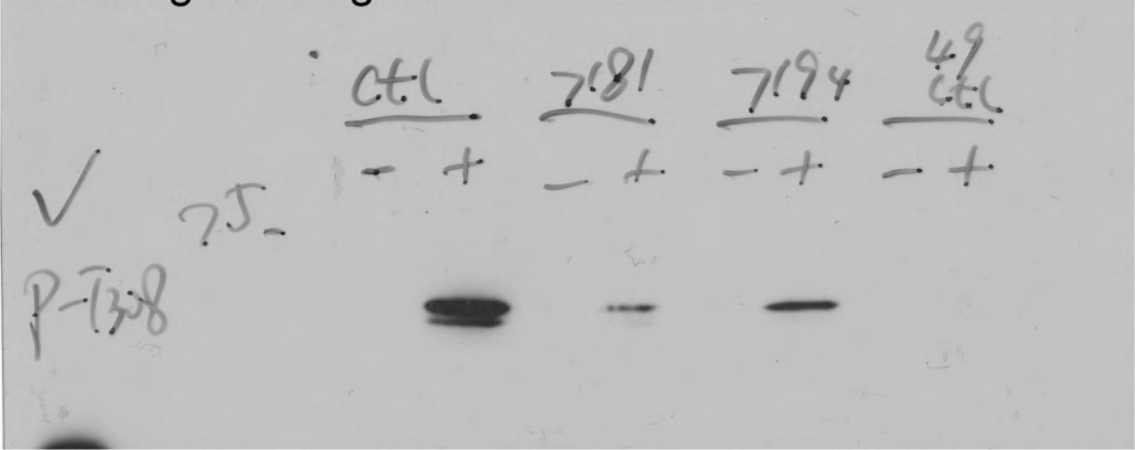
# Full unedited gel for Figure 4A



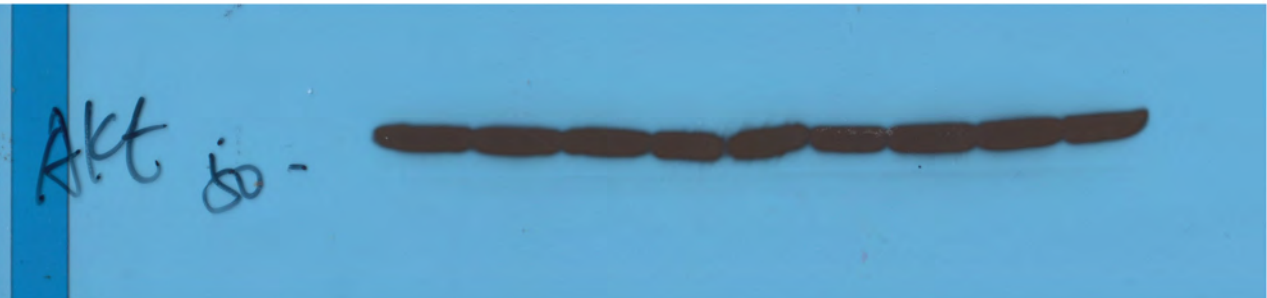
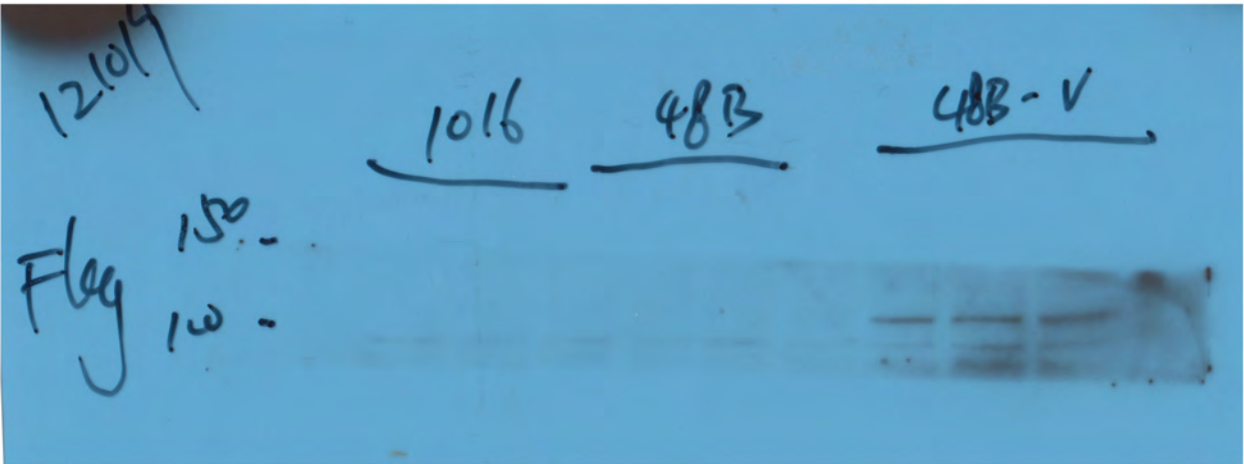
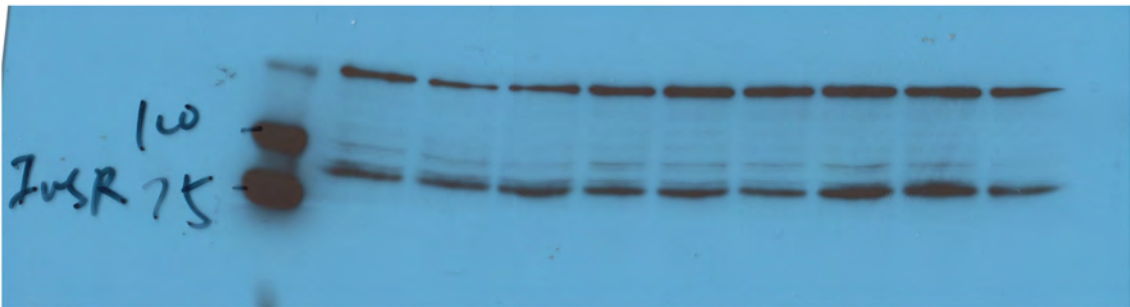
Full unedited gel for Figure 4C



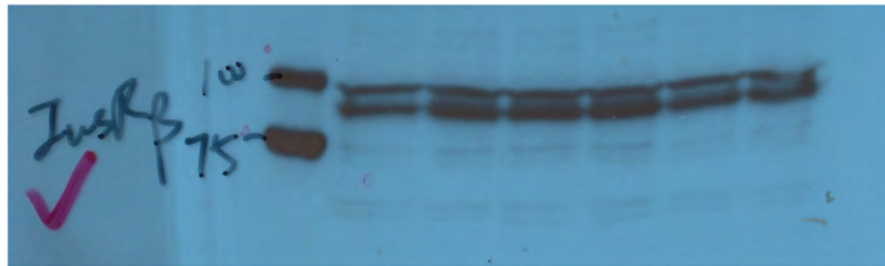
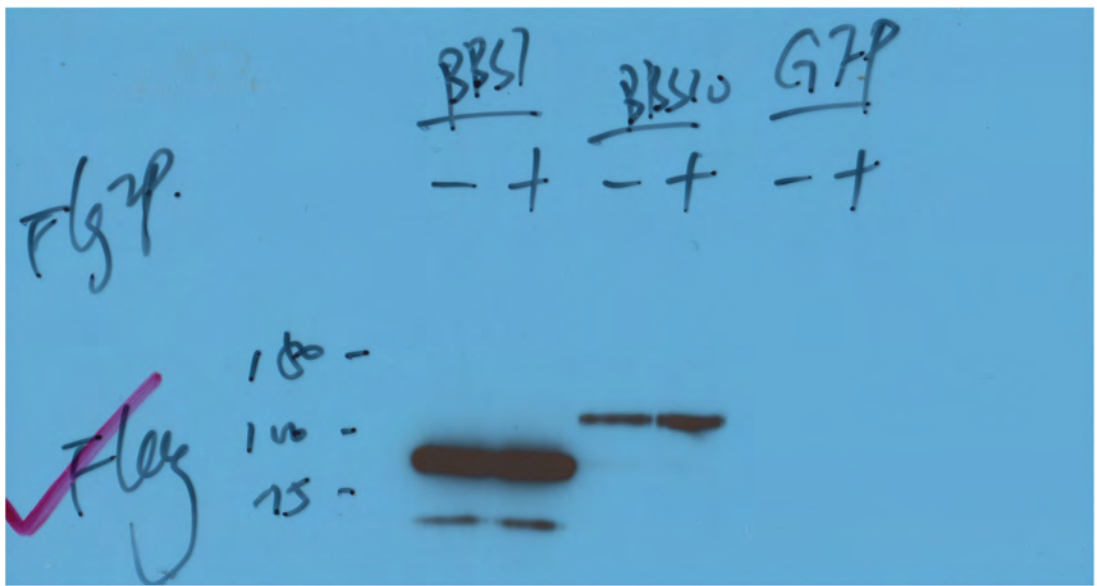
Full unedited gel for Figure 4E



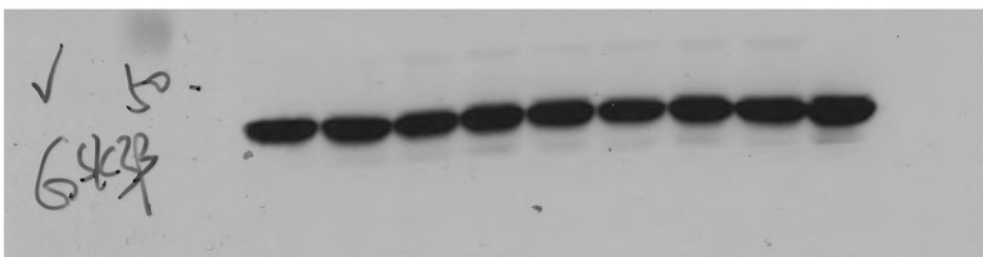
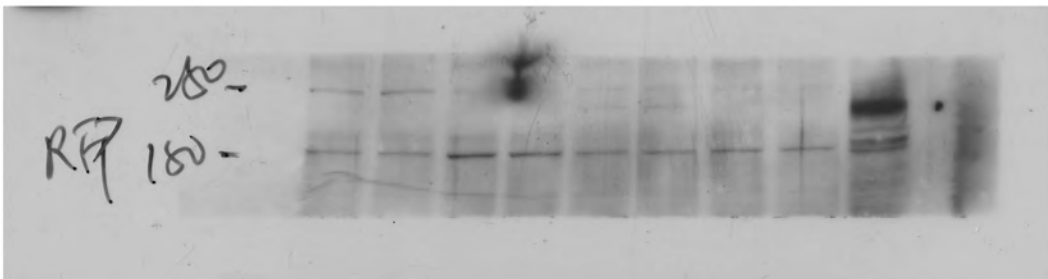
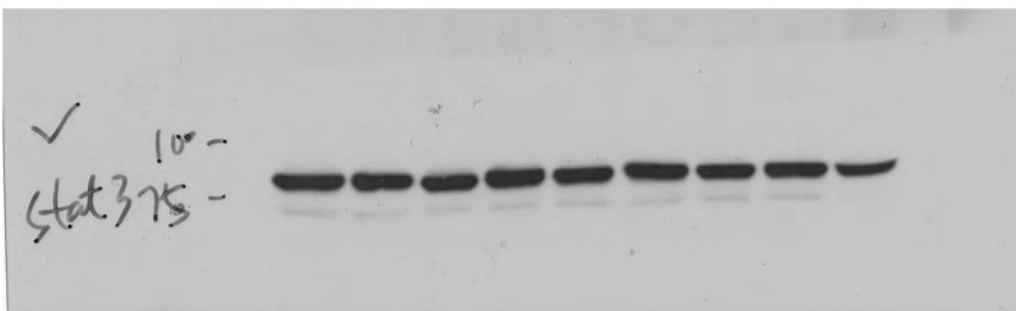
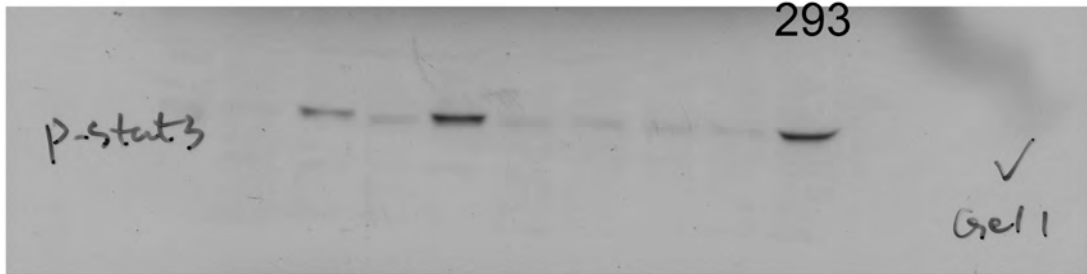
Full unedited gel for Figure 4G



Full unedited  
gel for  
Figure 4J

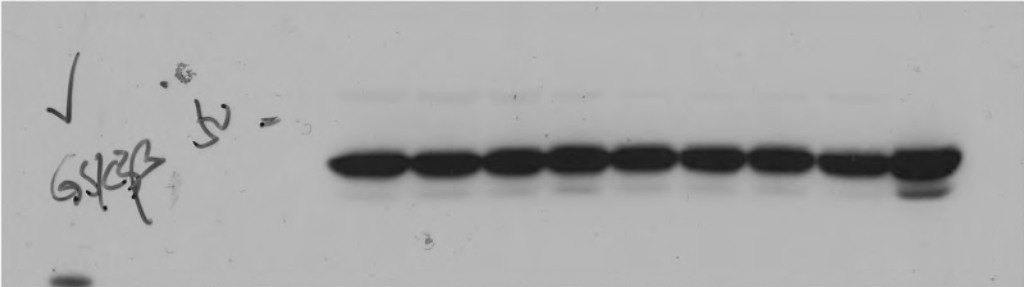
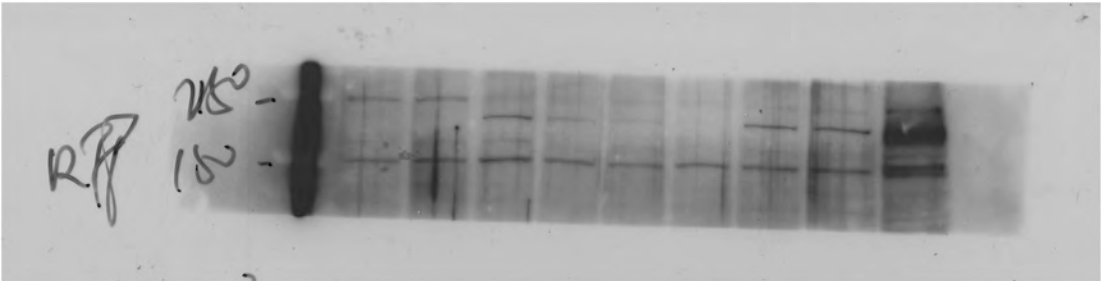
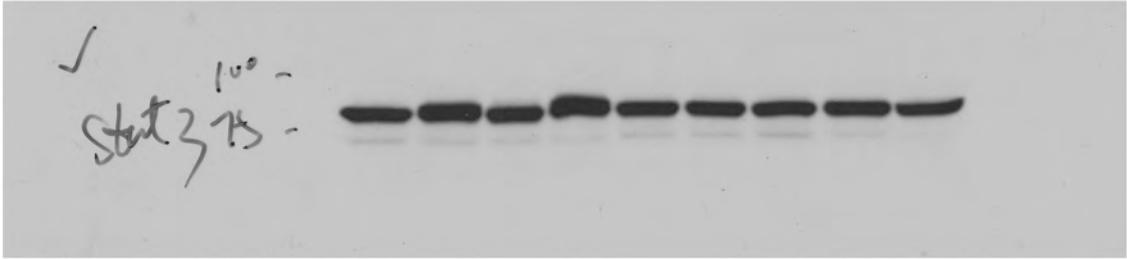
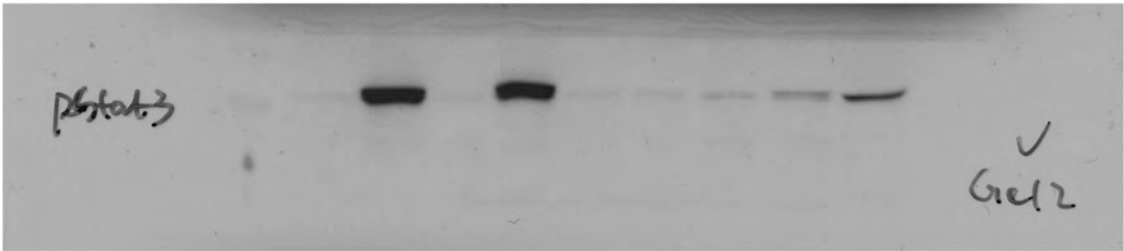


Full unedited gel for Figure 5A



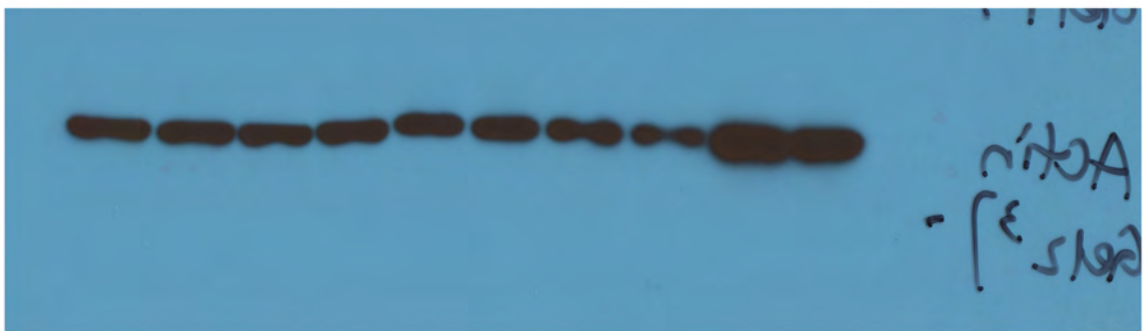
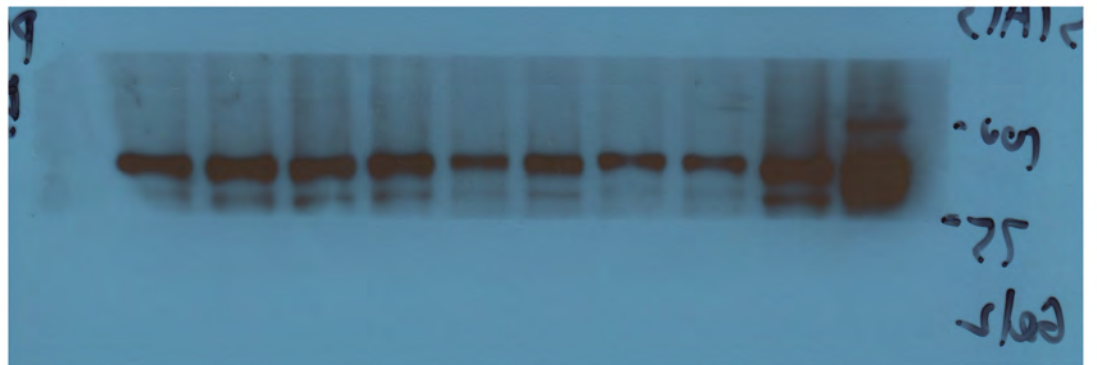
Full unedited gel for Figure 5C.

293

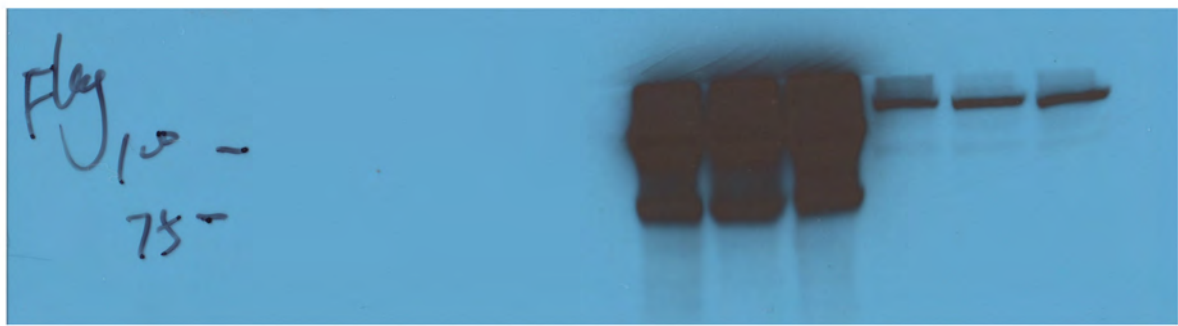
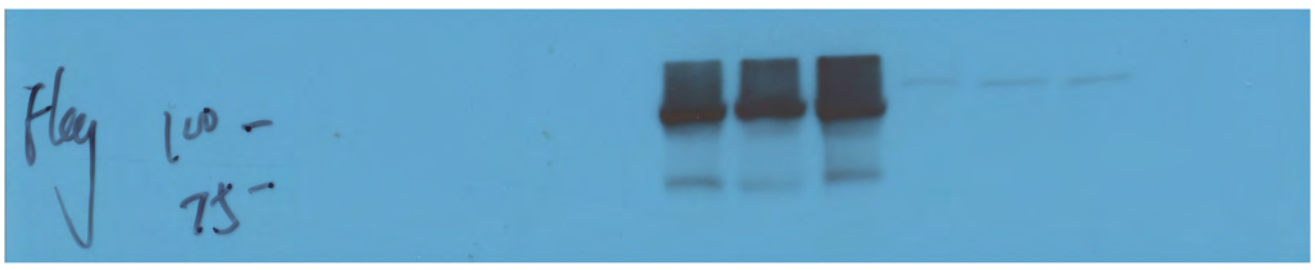
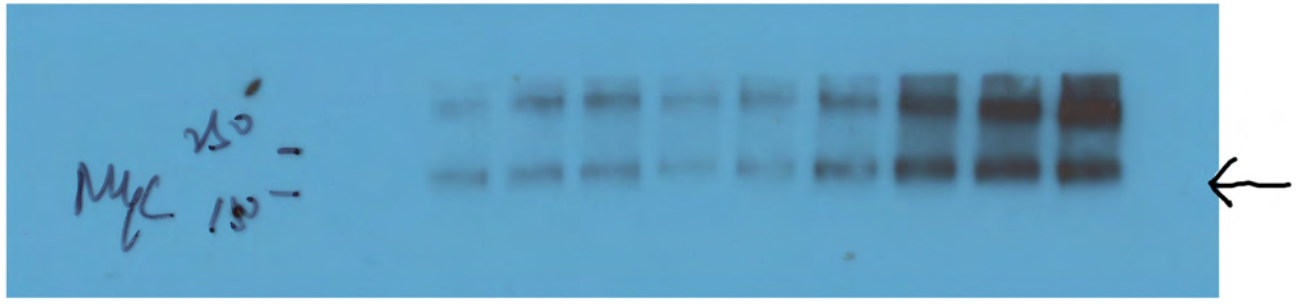


Full unedited gel for Figure 5F

CUT

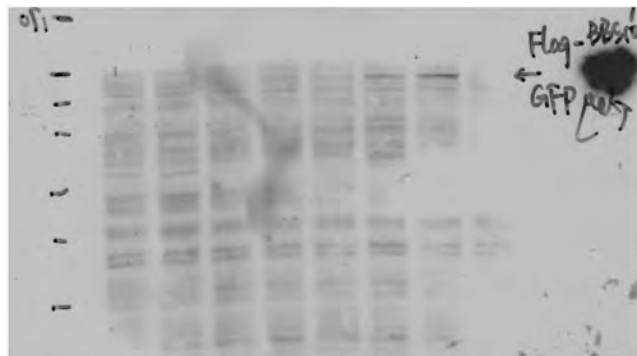


Full unedited gel for Figure 5K

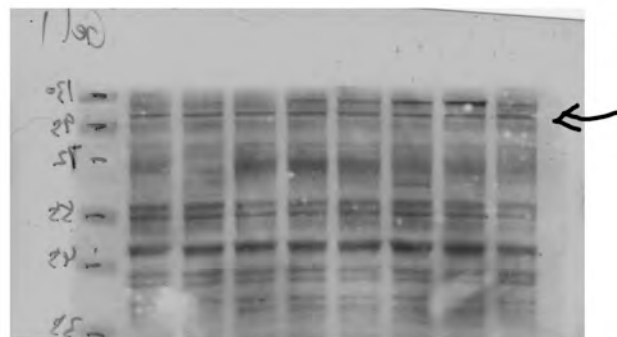


Full unedited gel for Figure S8C

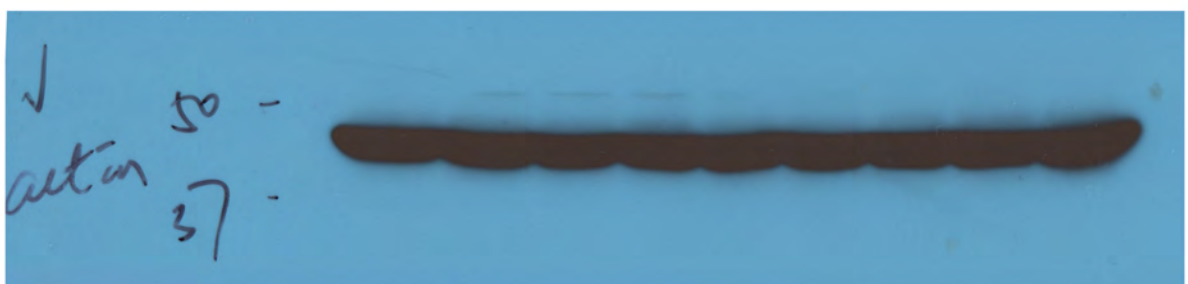
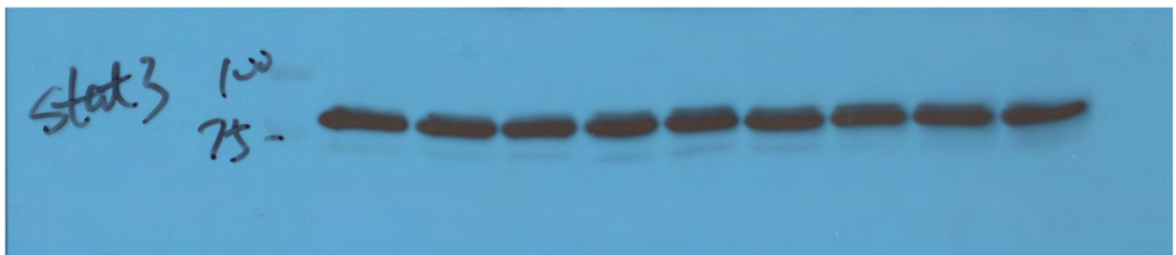
GFP



BBS10



Full unedited gel for Figure S15A



Full unedited gel for Figure S15E

